

Evaluating the Role of Mechanical Connections and Reinforcements in Modular Timber Beam Behaviour

Mohd Rizuwan Mamat^{1,3}, Mohd Hisbany Mohd Hashim^{1,4*}, Noorsuhada Md Nor^{2,5}

¹Faculty of Civil Engineering, Universiti Teknologi MARA, Shah Alam, Selangor, MALAYSIA

²Faculty of Civil Engineering, Universiti Teknologi MARA, Permatang Pauh, Pulau Pinang, MALAYSIA

³Forest Research Institute Malaysia (FRIM), Kepong, Selangor, MALAYSIA

⁴3R: Rehabilitation, Repair and Retrofitting Group, Faculty of Civil Engineering, Universiti Teknologi MARA, Shah Alam, Selangor, MALAYSIA

⁵Material and Structural Integrity Research Group, Civil Engineering Studies, Universiti Teknologi MARA, Permatang Pauh, Pulau Pinang, MALAYSIA

*Corresponding author: hisbany@uitm.edu.my

SUBMITTED 16 May 2025 REVISED 2 July 2025 ACCEPTED 25 July 2025

ABSTRACT Modular timber construction faces critical challenges in connection performance, with mechanical joints representing the weakest structural elements in segmented systems, particularly for rapid-deployment infrastructure applications such as temporary forest bridges. This research addresses the fundamental knowledge gap regarding the combined effects of mechanical connections and reinforcement strategies on modular timber beam structural behavior. The study investigates modular timber beam flexural performance through experimental evaluation of steel U-shaped connectors and Chopped Strand Mat (CSM) reinforcement applied to the tension zones, examining how beam segmentation affects structural integrity. Ten I-section modular timber beams with lattice-web configuration underwent three-point bending tests using a Shimadzu AG-IS 100 kN Universal Testing Machine at 6.6 mm/min loading rate, with specimens spanning 3.0 meters supported at 2.7-meter intervals. Test specimens featured varying segmentation patterns (0.6m, 0.75m, 1.0m, and 1.5m segment lengths) connected via U-shaped steel connectors and bolts, with selected beams receiving 5mm thick CSM reinforcement at the bottom flanges. Mechanical properties including modulus of elasticity (MOE), modulus of rupture (MOR), and flexural stiffness were systematically measured to quantify reinforcement and segmentation effects on joint behavior and structural continuity. Results demonstrate that CSM reinforcement provides substantial performance improvements, with ETR136 achieving a 49% increase in ultimate load capacity (29,397 N vs 19,709 N for ETN131) and superior ductility characteristics. However, segmentation introduces significant structural vulnerabilities, with five-segment beams (ETN50.65) showing a 49.5% capacity reduction compared to continuous specimens. The research reveals that while CSM reinforcement effectively delays crack initiation and reduces peak tensile strain by an average of 31%, mechanical joints remain critical failure points due to stress concentrations at the timber-bolt interfaces. The three-segment configuration emerges as optimal for balancing structural performance with practical modularity requirements. These findings provide essential design guidance for modular timber systems in rapid-deployment applications, emphasizing the need for optimized connection strategies and hybrid reinforcement techniques to enhance the structural integrity and durability of segmented timber infrastructure.

KEYWORDS Modular timber beams, Chopped Strand Mat, Stiffness degradation, Timber-bolt connections, Segmented beam behaviour

© The Author(s) 2026. This article is distributed under a Creative Commons Attribution-ShareAlike 4.0 International license.

1 INTRODUCTION

Modular construction provides enhanced efficiency and structural performance, with timber materials offering economical solutions for developing markets (Rahman et al., 2024). Research on modular systems demonstrates that beam-column connections significantly affect seismic performance (Boafo et al., 2016), load-bearing capacity (Wang et al., 2019), and structural behavior (Lee et al., 2020), establishing mechanical connections as critical performance determinants.

Modern timber frame construction heavily depends on timber-bolt connections. The United States, Canada, and Europe design codes classify these connections as pin joints (Shu et al., 2022). Research indicates that bolt connectors with ductile properties function effectively in timber and lightweight concrete composite beams because bending failure occurs before any other

failure mode (Hu et al., 2021). The cyclic loading of timber structures with conventional bolted connections results in decreased stiffness and strength, often manifesting as pinching effects in hysteresis loops.

Bolted connections in timber structures present complex simulation challenges (Karagiannis et al., 2016), though perpendicular reinforcement shows beneficial results (Okunrounmu et al., 2022). Research on timber frame behavior demonstrates that connection design determines structural performance (Liu and Xiong, 2018), while studies have analyzed connections under various loading scenarios, examining end distance and moisture content effects (Lokaj et al., 2020). However, timber-bolt connections in modular systems require further investigation.

Hu et al. (2021) examined timber-lightweight concrete composite beams with ductile bolt connectors to identify failure mechanisms and connection effectiveness. Manalo and Mutsuyoshi (2011) investigated mechanical joint behavior in fiber-reinforced composite beams under flexural loading, providing essential insights for connection performance in composite systems. Both studies address segmentation optimization in hybrid material systems, where mechanical connections govern stress transfer and determine the balance between modular flexibility and structural performance, which is directly relevant to CSM-reinforced timber systems.

Recent studies have examined ductile moment-resisting timber joints for energy dissipation (Rebouças et al., 2022) and axial behavior of steel-laminated timber connections (Shi et al., 2023). Research has investigated various connection characteristics including fire performance, bolt connectors, and loading conditions (Okunrounmu et al., 2022; Hu et al., 2021; Liu and Xiong, 2018), though flexural bending behavior requires further investigation. Extensive research on modular timber beam flexural strength has focused on bolt spacing (Yang et al., 2020), bolt loosening under transverse loads (Chen et al., 2020), and load-slip behavior under bending conditions. However, additional investigation is needed into the flexural bending response of modular timber beams with and without reinforcement. This study examines the flexural characteristics of modular timber beams through segment length analysis and mechanical connection assessment. Ten beams with varying configurations were evaluated, with selected specimens receiving Chopped Strand Mat (CSM) reinforcement.

2 METHODS

2.1 Preparation of Modular Timber Beams

The experimental specimens consisted of I-shaped modular timber beams (as shown in Table 1). The beams consisted of two timber flanges, which were connected by a lattice-patterned web. The beams were de-

signed to transfer loads efficiently while minimizing their weight. The beam sections had a width of 80 millimetres and a height of 240 millimetres with lengths spanning from 0.6 meters to 3.0 meters.

The segmental assembly used U-shaped steel connectors together with high-strength bolts to connect beam modules and employed a system-level experimental approach to evaluate segmented versus continuous modular timber beam performance. The primary objective was quantifying how segmentation affects overall structural behavior (deflection, stiffness, load capacity) rather than isolating connection positioning effects. Connection locations were geometrically determined by segmentation patterns and represented realistic modular configurations. Denting corrections were systematically applied to ensure comparable deflection measurements between specimens in which loading contacted timber versus connector surfaces, enabling valid system-level comparisons. The experimental approach recognizes that connection positioning represents a secondary effect compared to the dominant influence of segmentation level on system performance. This system-level methodology provides practical guidance for segmentation strategy selection while acknowledging that connection stress variations are inherent to modular configurations but do not significantly alter the primary findings regarding segmentation effects.

To enhance tensile resistance in selected beams, a CSM reinforcement layer, 5 mm thick and impregnated with epoxy resin, was applied to the tension zone (i.e., the bottom flange) of specific specimens. This layer was uniformly distributed along the lower flange to improve tensile strength, delay crack initiation, and reduce stiffness degradation under flexural stress. The reinforcement technique aimed to create a composite action between the timber and CSM layer, thereby enhancing the strength-to-weight ratio and resistance to deformation. The improved ductility and reduced susceptibility to cracking contributed significantly to the structural performance of the beams.

Table 1. Summary of specimen configurations including CSM reinforcement, segment count, and segment lengths

Specimen ID	CSM Reinforcement	Number of Segments	Segment Length (m)
ETN131	No	1 (continuous)	3.00
ETN21.52	No	2	1.50
ETN313	No	3	1.00
ETN40.754	No	4	0.75
ETN50.65	No	5	0.60
ETR136	Yes (5 mm)	1 (continuous)	3.00
ETR21.57	Yes (5 mm)	2	1.50
ETR318	Yes (5 mm)	3	1.00
ETR40.759	Yes (5 mm)	4	0.75
ETR50.610	Yes (5 mm)	5	0.60

A total of ten beams were fabricated and divided into two main groups: unreinforced and CSM-reinforced. The unreinforced group (ETN131, ETN21.52, ETN313, ETN40.754, ETN50.65) relied solely on the inherent mechanical properties of timber and the structural efficiency of the lattice web (as shown in Figure 1). The ETN131 specimen, in particular, was constructed without any joint or reinforcement elements, providing a baseline for comparison. The triangular lattice geometry facilitated uniform load distribution along the span, thereby enhancing bending resistance.

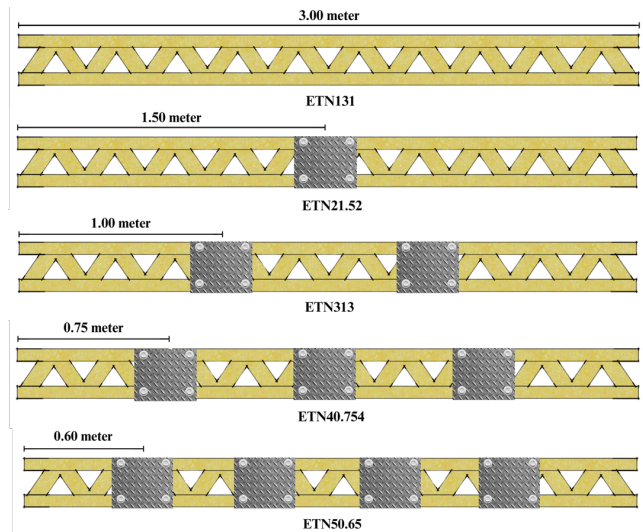


Figure 1 Modular timber beam unreinforced with chopped strand mat.

The reinforced group (ETR136, ETR21.57, ETR318, ETR40.759, ETR50.610) included beams with CSM reinforcement applied to their lower flanges and joined via bolted metal plates (as shown in Figure 2). These specimens were expected to demonstrate improved flexural behavior, including higher stiffness, reduced deflection, and delayed onset of plastic deformation when subjected to bending.

2.2 Connection Design Verification

The mechanical connectors were specifically designed to handle both static and dynamic loads and playing an essential role in transmitting loads between beam segments. The bolts served dual roles by withstanding both shear and tensile forces while maintaining joint integrity. The mechanical assembly included beam specimens labeled ETN21.52, ETN313, ETN40.754, ETN50.65, ETR21.57, ETR318, ETR40.759, and ETR50.610, all connected using bolted metal plates to ensure efficient force transfer and structural continuity across interfaces of the modular timber beam.

The U-shaped steel connectors were specifically designed to handle both static and dynamic loads through comprehensive capacity verification. Design calcu-

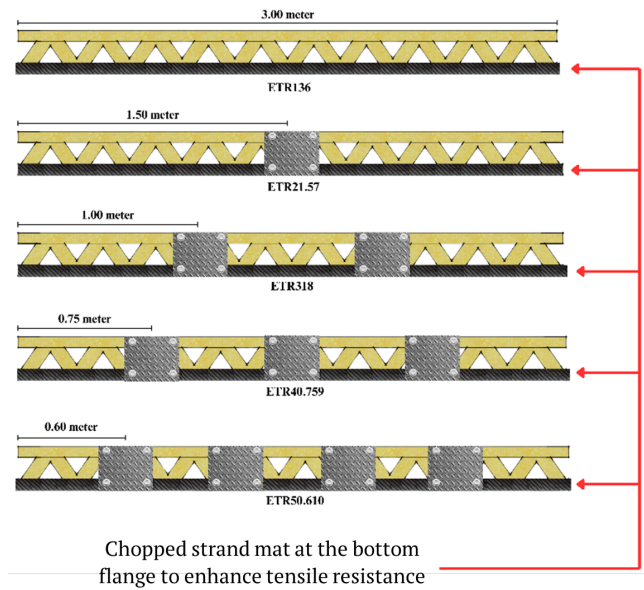


Figure 2 Modular timber beam reinforced with chopped strand mat applied at bottom flange.

lations were based on the critical loading condition of ETR318 (three-segment reinforced configuration) which achieved 13,078 N maximum load.

Internal force analysis determined a critical shear force of $V = 6,539$ N at connection locations, resulting in 1,635 N load per bolt when considering the 4-bolt pattern and uneven load distribution observed in experimental testing. Bolt capacity verification for Ø10mm high-tensile galvanized steel showed 26.0% shear capacity utilization when accounting for experimentally observed stress concentration factors of 3.0.

Bearing stress analysis revealed timber bearing utilization of 49.2% (safety factor 2.03) and steel bearing utilization of 39.2% (safety factor 2.55), confirming adequate capacity margins. The experimental validation showed 62.5% efficiency between theoretical capacity (20,944 N) and achieved performance (13,078 N), reflecting real-world complexity such as stress concentrations and load redistribution effects documented through bolt deformation analysis.

2.3 Test Set-up

A comprehensive experimental setup in this study aims to assess the flexural strength and rigidity of modular timber beams through three-point bending tests on reinforced and non-reinforced beams with CSM in the tension zone. This research focuses on evaluating modular girder concepts for portable bridge applications, where segmentation represents the primary design parameter under investigation. Three-point bending was selected to provide consistent midspan peak moment conditions across all specimen configurations,

enabling direct comparison of segmentation effects on structural performance. This methodology ensures that all specimens are evaluated under the same critical loading condition that governs girder performance in portable bridge applications, providing a standardized basis for assessing both segmentation effects and reinforcement effectiveness, regardless of segmentation level or reinforcement configuration applied to the specimen.

The research evaluated essential parameters including MOE, MOR and load-deflection response to enable performance assessments between different configurations. The Shimadzu AG-IS 100 kN Universal Testing Machine operated as the experimental testing device for three-point bending tests. The timber beam specimens rested on rigid steel supports which were placed 2.7 meters apart to create a simply supported boundary condition. The supports were positioned 150 mm away from each beam end to maintain uniform test conditions throughout all samples. A cylindrical steel loading head with a 28 mm diameter served as the central point for applying vertical loads. The testing setup duplicated real-world structural bending and shear effects while reducing stress concentrations at the loading point. Tests were conducted in displacement control mode at 6.6 mm/min using the Shimadzu AG-IS 100 kN Universal Testing Machine in accordance with ASTM D198 procedures.

Deflection data were collected in real time using Linear Variable Differential Transformers (LVDTs) installed at midspan and critical points along the span. Additionally, strain gauges were affixed to the top and bottom flanges to capture compressive and tensile strain responses, respectively. This dual monitoring approach provided insight into stress distribution, stiffness loss, and the role of reinforcement under flexural action.

Failure modes were visually and quantitatively documented, including tensile rupture in the bottom flange, compression-induced buckling in the top flange, and localized failures at mechanical joints. Special attention was given to the behavior of bolted connectors under increasing flexural demands. The experimental procedures conformed to ASTM D198 (ASTM International, 2021a) bending tests and ASTM D5652 (ASTM International, 2021b) for evaluating joint behavior. These standards ensured methodological consistency and allowed for rigorous, reproducible comparisons between reinforced and unreinforced modular timber beams. Key mechanical properties were derived from the recorded data of a) Modulus of elasticity (E) which is calculated from the elastic region of the load-deflection curve, offering insights into beam stiffness b) Stiffness evaluation from deflection data at specific load levels was analyzed to compare the performance of beams with and without CSM reinforcement.

The modulus of elasticity was determined using the standard three-point bending test Equation (1) (ASTM International D198, 2021) as follows:

$$E = \frac{PL^3}{48 I \delta} \quad (1)$$

Where, P is applied load (N), L is the beam span (mm), I is the moment of inertia (mm^4), and δ is mid-span deflection (mm). To assess the stiffness degradation over repeated loading cycles, the stiffness degradation index (SDI) was calculated using Equation (2):

$$SDI = \frac{k_{\text{initial}} - k_{\text{final}}}{k_{\text{initial}}} \times 100\% \quad (2)$$

Where k_{initial} and k_{final} represent stiffness values calculated from the first and final segments of the load-deflection curve, respectively. The SDI calculation employs a systematic 10-segment approach where each load-deflection curve is divided into 10 equal segments based on the total deflection range. Initial stiffness (k_{initial}) is calculated from the first segment representing early loading response, while final stiffness (k_{final}) is calculated from the tenth segment representing late-stage behavior. Positive SDI values indicate stiffness degradation, while negative SDI values indicate progressive stiffness enhancement due to reinforcement engagement, where k_{final} exceeds k_{initial} as CSM reinforcement becomes increasingly effective at sharing tensile loads during loading.

3 RESULTS

3.1 Load-deflection of Unreinforced Modular Timber Beams

The unreinforced modular timber beams exhibited distinct mechanical responses under flexural loading, characterized by variations in stiffness retention, maximum load capacity, and failure behavior. All specimens initially followed a linear elastic trend, in which midspan deflection increased proportionally with the applied load, indicating elastic deformation governed by the timber material and lattice web configuration.

As loading progressed beyond the elastic limit, as shown in Figure 3, divergence in flexural performance was observed across different beam types. The beam specimen ETN131 (3m \times 1 segment), constructed without any mechanical joints, demonstrated the highest maximum load capacity of 19,709 N, reflecting the efficiency of uninterrupted material continuity in load transfer. In contrast, ETN50.65 (0.6m \times 5 segments), which was comprised multiple bolted segments, recorded the lowest maximum load at 9,956 N, indicating that mechanical discontinuities contributed to stress concentrations and early stiffness degradation.

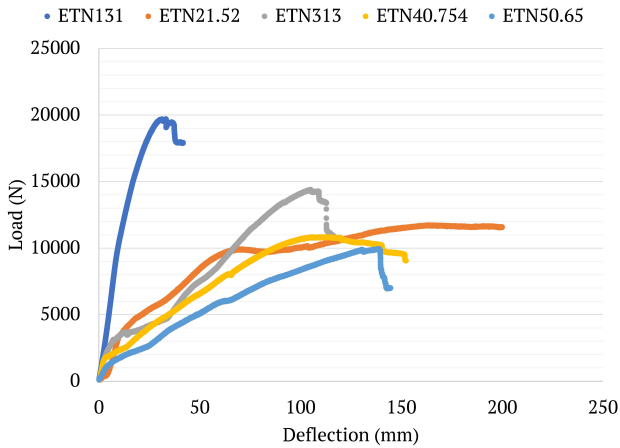


Figure 3 Load-deflection relationships for all unreinforced modular timber beams.

Intermediate specimens such as ETN313 (1m \times 3 segments) and ETN21.52 (1.5m \times 2 segments) reached maximum load capacities of 14,403 N and 11,728 N, respectively, exceeding that of ETN40.754 (0.75m \times 4 segments) at 10,844 N, but exhibited pronounced post-yield stiffness reduction. This suggests that although these beams could carry relatively higher loads, their ability to sustain structural rigidity diminished rapidly after initial yielding. The post-peak behavior varied significantly among samples, with ETN313 showing a sharp decline after reaching its maximum load capacity, indicating rapid connection shear failure with immediate load loss, while ETN40.754 demonstrated a more gradual decline in load-carrying capacity.

A particularly notable response was observed in ETN21.52, which displayed an extended plateau region in the load-deflection curve. This behavior indicates of improved energy dissipation, potentially resulting from enhanced stress redistribution at the bolted joints that delayed the onset of sudden connection failure and structural discontinuity. Unlike the other segmented beams, ETN21.52 maintained a relatively constant load despite increasing deflection, demonstrating superior ductility in its post-peak phase. This suggests that the two-segment configuration with 1.5m segments may offer an optimal balance between modularity and structural integrity.

Across all specimens, timber-bolt connections were consistently identified as critical failure points. Common issues included stress concentrations at connector points, bolt bending and deformation (particularly at central connectors), and localized material yielding with connector slippage. These connection vulnerabilities significantly impacted the overall structural performance and failure modes of the segmented beams.

Figure 4 shows that the analysis of segmented beam specimens comprising 2 to 5 segments indicated that

non-reinforced beams achieved a higher average maximum load capacity (11,733 N) compared to their reinforced counterparts (10,834 N). This finding suggests that segmentation introduces greater performance degradation in reinforced beams, likely due to stress concentrations and potential delamination effects at the mechanical joints. Furthermore, the average maximum load capacity of the segmented non-reinforced beams exhibited a significant reduction compared to the full-length unreinforced control specimen ETN131 (19,709 N), underscoring the detrimental impact of segmentation on load-carrying capacity. These results highlight that segmenting timber beams without reinforcement leads to a pronounced loss in stiffness and structural efficiency, with a general trend of more segments correlating with more rapid failure progression and reduced energy dissipation capacity due to the additional connection points where stress concentrations develop.

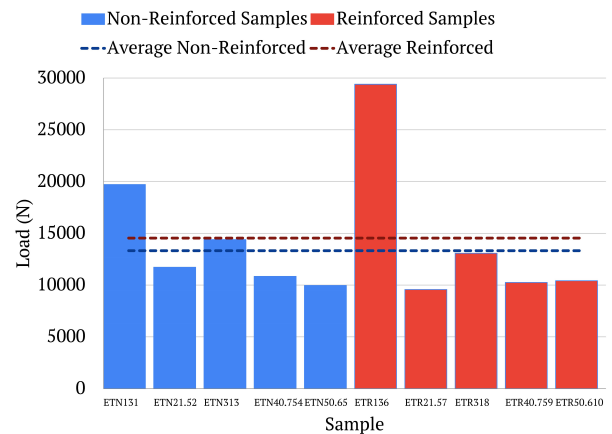


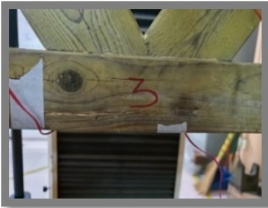
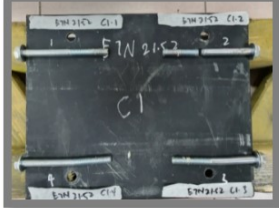
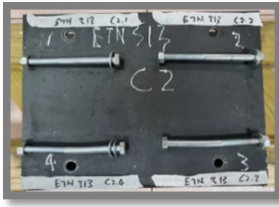
Figure 4 Maximum loading for all reinforced and unreinforced modular timber beams.

3.2 Failure Modes of Unreinforced Modular Timber Beams

Table 2 shows that the visual inspection of the tested specimens identified critical failure zones concentrated at mechanical connection interfaces, where localized stress accumulation led to bolt deformation and timber fracturing. In ETN131, longitudinal cracking along the grain and fiber crushing adjacent to bolt holes were observed indicating significant stress concentrations and material crushing under compressive forces. ETN21.52 exhibited pronounced bolt bending and visible washer wear, suggesting fatigue-induced degradation at the connection points due to repeated stress cycling. In contrast, ETN313 and ETN50.65 experienced rapid connection shear failure at peak load, marked by severe bolt distortion, connector slippage, and loss of structural continuity that indicated limited ductility and inadequate energy dissipation. Meanwhile, ETN40.754

displayed a more progressive stiffness reduction before complete structural discontinuity, likely due to improved stress redistribution at the joints, which temporarily delayed the initiation of connection failure relative to other unreinforced segmented beams.

Table 2. Failure modes of the unreinforced modular timber beams

Failure modes	Failure modes on bolts
ETN131	ETN131
	
ETN21.52	ETN21.52
	
ETN313	ETN313
	
ETN40.754	ETN40.754
	
ETN50.65	ETN50.65
	

3.3 Load-deflection of Reinforced Modular Timber Beams

Figure 5 shows the load-deflection behavior of reinforced modular timber beams with CSM applied in the tension zone. The incorporation of CSM reinforcement into modular timber beams significantly enhanced their structural performance, as evidenced by increased load-bearing capacity, reduced stiffness degradation, and improved post-yield ductility. All samples exhibited distinct behavioral phases: an initial elastic phase with high stiffness and a linear load-deflection relationship, followed by a transition phase from elastic to plastic deformation, and finally a post-peak behavior that varied significantly between samples.

Reinforced beams demonstrated higher initial stiffness and a more extended plastic deformation phase compared to their unreinforced counterparts. Among all specimens, ETR136 (3m × 1 segment) achieved the highest maximum load capacity of 29,397 N, representing a 49% increase over the full-length unreinforced beam ETN131 (19,709 N), thereby validating the effectiveness of bottom-flange reinforcement in resisting flexural stresses. The control sample ETR136 also exhibited the most favorable post-peak response, showing only gradual stiffness degradation with force decreasing from approximately 28,000 N to 26,000 N, indicating superior energy absorption and structural integrity.

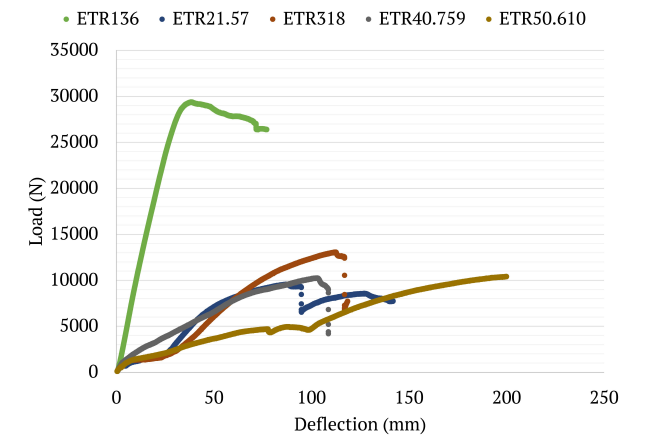


Figure 5 Load-deflection relationships for all reinforced modular timber beams with CSM.

Reinforced beams ETR318 (1m × 3 segments) and ETR50.610 (0.6m × 5 segments) also exhibited enhanced energy dissipation, attaining peak loads of 13,078 N and 10,422 N, respectively, accompanied by delayed failure and improved ductility. ETR318 performed best among the segmented samples in terms of maximum load capacity; however, it experienced catastrophic failure with a steep decline after reaching its peak load. In contrast, ETR50.610 demonstrated su-

perior post-peak behavior by maintaining consistent load-carrying capacity despite significant deflection (up to $\sim 0.2\text{m}$), suggesting better ductility and residual strength characteristics. These behaviors suggest that the composite interaction between the CSM layer and timber substrate contributed to a more controlled failure mode, minimizing brittle fracture and connector-induced stress concentrations.

However, ETR21.57 ($1.5\text{m} \times 2$ segments), despite being reinforced, recorded a relatively low maximum load capacity of 9,578 N, followed by a sharp load drop to approximately 6,500 N after reaching maximum load capacity, highlighting the persistent influence of mechanical joint weaknesses. ETR40.759 ($0.75\text{m} \times 4$ segments) reached a peak load of 10,259 N before experiencing a sharp decline, though it maintained some residual capacity between 4,000–7,000 N. These variations suggest that while CSM reinforcement improves overall performance, the effectiveness of the system remains sensitive to connector detailing and load redistribution efficiency at segmental interfaces.

The CSM reinforcement effectively delayed crack initiation and propagation, particularly in tensile areas, distributed tensile forces more evenly across beams, and provided residual load-carrying capacity even after primary failure. However, despite reinforcement, timber-bolt connections remained critical failure points, with stress concentrations at connector locations (particularly C1, C2, and C3) and bolt bending under high loads limiting overall beam performance.

It was found that the segmented beams with reinforcement shown earlier in Figure 4 exhibited a lower average maximum load (10,834 N) compared to their non-reinforced counterparts (11,733 N). The dramatic decrease in load capacity from the control (29,397 N) to segmented samples (9,578–13,078 N) confirms that reinforcement alone is insufficient to overcome the structural weaknesses introduced by segmentation, particularly those associated with stress concentrations and discontinuities at mechanical joints. This finding suggests that optimal structural behavior requires both effective reinforcement and improved connection designs, particularly in modular/segmented applications.

3.4 Failure Modes of Reinforced Modular Timber Beams

Beams ETR136 and ETR318 as presented in Table 3 exhibited a progressive failure pattern, primarily attributed to the gradual propagation of cracks, demonstrating the efficacy of CSM reinforcement in enhancing structural performance. This reinforcement effectively distributed stress, enabling the beams to sustain higher loads before significant deformation occurred. In contrast, ETR21.57 experienced rapid bearing failure around bolt holes despite reinforcement, indicat-

Table 3. Failure modes of the reinforced modular timber beams

Failure modes	Failure modes on bolts
ETR131	ETR131
	
ETR21.52	ETR21.52
	
ETR313	ETR313
	
ETR40.754	ETR40.754
	
ETR50.65	ETR50.65
	

ing that high stress concentrations around the bolt locations remained a critical vulnerability, leading to an immediate loss of load-carrying capacity. Conversely, ETR40.759 and ETR50.610 maintained their capacity to bear residual loads after reaching their peak capacity, suggesting that CSM reinforcement contributed to improved tensile stress distribution. This enhancement allowed the beams to resist rapid structural degradation and maintain their structural integrity for extended periods under continuous loading.

3.5 Stiffness Degradation

The comparative analysis between reinforced and non-reinforced modular timber beams revealed the complex interplay between reinforcement benefits and segmentation effects. The performance data are presented in Table 4. Reinforced beams demonstrated a higher average maximum load capacity of 14,547 N compared to 13,328 N for non-reinforced specimens, representing a 9.1% improvement overall. This enhancement is attributed to the CSM reinforcement's ability to redistribute tensile stresses more effectively along the bottom flange, allowing the beams to withstand greater bending moments before material failure. However, a surprising phenomenon emerged when specifically examining segmented beams (comprising 2 to 5 segments): non-reinforced modular timber beams outperformed their reinforced counterparts with average peak loads of 11,733 N versus 10,834 N for reinforced segmented specimens. This 8.3% performance reduction in reinforced segmented beams can be attributed to several mechanical factors including discontinuity effects, stress amplification, load path disruption, and interface compatibility issues.

The reinforcement layer creates a stiffer composite section that is more adversely affected by the discontinuities at mechanical joints, while the higher stiffness of reinforced sections causes greater stress concentration at bolt interfaces when segmented. Additionally, mechanical joints interrupt the continuous load transfer through the reinforcement, negating much of its benefit, and differences in elastic properties between timber, reinforcement, and steel connectors create complex stress states at segment boundaries. This counterintuitive finding highlights that segmentation introduces a more pronounced weakening effect in reinforced beams, primarily due to the incompatibility between reinforcement continuity and mechanical joint behavior.

In terms of stiffness performance, reinforced beams demonstrated superior retention of stiffness, with

some specimens even exhibiting negative stiffness degradation—suggesting a net gain in rigidity during loading. Stiffness degradation for reinforced beams ranged from −34% to 46%, whereas non-reinforced beams experienced more severe deterioration, with values between 7.6% and 74.8%. The specimen ETR136 exhibited the most notable improvement, achieving a −2.4% change in stiffness, in contrast to its non-reinforced counterpart ETN131, which showed a 7.6% degradation. The negative SDI values in ETR318 and ETR136 indicate progressive stiffness enhancement during loading rather than degradation. This occurs as micro-cracking in the timber matrix causes the CSM reinforcement to become increasingly effective at sharing tensile loads, creating composite action that actually improves system stiffness as loading progresses. These findings support the conclusion that CSM reinforcement significantly mitigates stiffness loss, particularly in less segmented or full-length beams. However, reinforced segmented specimens, such as ETR40.759 and ETR50.610, still recorded considerable stiffness degradation (46.1% and 41.5%, respectively), reaffirming that mechanical joints remain critical zones of vulnerability.

Despite the enhancements provided by reinforcement, failure patterns across both beam groups were predominantly influenced by stress concentrations at mechanical interfaces, with frequent occurrences of rapid connection failure, bolt slippage, and localized fracturing, especially in highly segmented designs. For modular bridge applications, the 3-segment configuration emerged as the optimal balance between structural performance and practical modularity. This configuration (represented by ETN313 and ETR318) demonstrated several advantages, including superior load capacity, moderate stiffness loss, transport efficiency, assembly practicality, and optimal performance-to-weight ratio.

The 3-segment design exhibited the highest load-bearing capacity among segmented options (14,403 N and 13,078 N respectively) while maintaining more manageable stiffness degradation compared to 4 and 5-

Table 4. Summary of specimen configurations including CSM reinforcement, segment count, and segment lengths

Specimen ID	Maximum Load (N)	MOR (MPa)	Calculated MOE (GPa)	Failure Mode	SDI (%)
ETN131	19709.380	17.323	5.954	Timber crushing at load point	7.58
ETN21.52	11728.120	10.308	0.535	Progressive bolt bending	46.46
ETN313	14403.120	12.659	1.042	Rapid connection shear	74.77
ETN40.754	10843.750	9.531	0.740	Timber splitting + bolt hole elongation	48.53
ETN50.65	9956.250	8.751	0.544	Multiple connection failure	29.39
ETR136	29396.880	25.873	7.564	Gradual crack propagation	-2.37
ETR21.57	9578.125	8.418	0.819	Bearing failure despite CSM	5.30
ETR318	13078.130	11.495	0.882	Connection failure + CSM delamination	-34.03
ETR40.759	10259.370	9.017	0.743	Progressive timber cracking	46.10
ETR50.610	10421.880	9.160	0.391	Controlled failure with bridging	41.53

segment designs. From a practical perspective, 1-meter segments are manageable for field transportation in forest environments, and fewer connection points reduce assembly complexity and potential failure zones. For implementing modular timber bridges, the recommendation is to utilize a 3-segment configuration with enhanced connection design, including reinforced bolt areas, larger diameter fasteners, and additional CSM reinforcement specifically at joint interfaces. This approach capitalizes on the benefits of CSM reinforcement while addressing the weakest link in the structural system, namely the mechanical connections that ultimately govern overall performance and longevity in field applications.

3.6 Strain Distribution

Strain measurements provided critical insights into the deformation behavior and stress distribution within segmented modular timber beams subjected to flexural loading. In non-reinforced beams, strain readings at the web region showed a progressive reduction from $216.85 \mu\epsilon$ in single-segment specimens to $-3.53 \mu\epsilon$ in four-segment beams as shown in Figure 6. This transition to negative strain indicates a significant stress redistribution around the mechanical connection zones, highlighting these joints as primary locations for stress concentration and potential instability. Additionally, strain measurements at the top flange remained relatively low, with intermittent negative values observed, particularly near segment interfaces, which suggests localized compression-induced instability and the potential early onset of failure under sustained loading conditions.

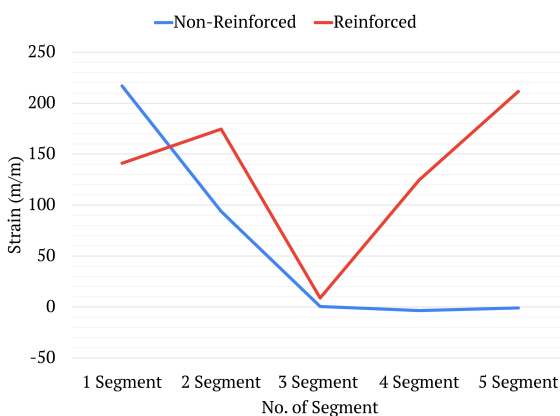


Figure 6 Strain distribution at the web of the beams.

In contrast, reinforced beams with CSM exhibited markedly lower and more stable strain responses across both the web and flange regions (as shown in Figure 7). Notably, specimens such as ETR136 and ETR318 recorded significantly reduced strain values at the web compared to their non-reinforced counterparts, reflect-

ing the reinforcement's capacity to distribute tensile stresses more uniformly. Furthermore, strain readings along the top flange in reinforced beams showed reduced fluctuation and better consistency, indicative of improved bending behavior and structural stability.

These findings affirm the role of CSM reinforcement in mitigating strain localization, reducing the magnitude of stress gradients across segment interfaces, and enhancing the overall integrity and deformation control of modular timber beams under flexural loads. The reinforcement effectively suppresses the formation of critical strain zones, particularly at mechanical joints, thereby delaying failure mechanisms associated with stress concentration in segmented systems.

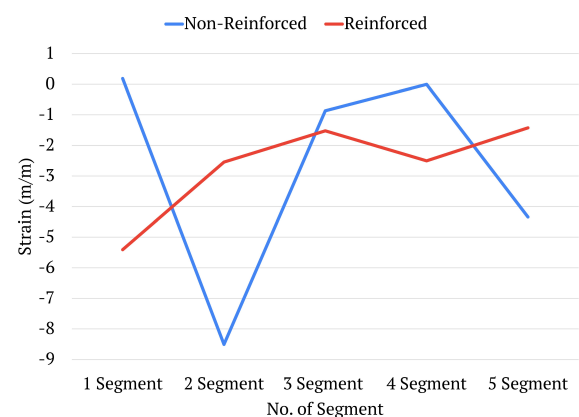


Figure 7 Strain distribution at the top flange of the beam.

4 DISCUSSION

The research evaluated modular timber beam flexural performance through an examination of mechanical joints, segment length, and CSM reinforcement effects on structural behavior. The experimental findings revealed that reinforced and non-reinforced beams exhibited different levels of stiffness degradation and ultimate load capacity and failure mechanisms. The CSM reinforcement according to Mirski et al. (2021) successfully extended crack propagation time and improved energy absorption but the segmentation process created structural weaknesses that mainly affected mechanical joint interfaces. The research demonstrated that modular systems require advanced connection methods for building portable infrastructure such as temporary forest bridges (Wdowiak-Postulak et al., 2024).

Structural performance was highly dependent on segment length. The study confirmed findings by Kržan et al. (2023) that mechanical connectors cause significant stiffness loss, with non-reinforced segmented beams losing up to 30% of their stiffness compared to full-length specimens. These findings align with the

result of dynamic analysis showing that increased segmentation correlates with decreased natural frequencies due to enhanced flexibility and reduced stiffness in modular timber systems (Mamat et al., 2025). The stiffness retention of reinforced beams remained better than that of non-reinforced beams because their stiffness degradation fell between 18–22% according to Wdowiak-Postulak (2020). The most significant stiffness reductions occurred in the shortest segmented beams (ETN50.65 and ETR50.610), because stress concentrations at joint interfaces likely accelerated failure initiation (Franke et al., 2015).

The evaluation of failure behavior between different mechanical joints revealed their restricted capabilities. The failure of non-reinforced beams initiated at connection interfaces where they exhibited rapid load loss with minimal post-peak capacity while showing minimal energy absorption and their stiffness decreased between 25% and 30%. The maximum load-bearing capacity of beams ranged between 9,956 N and 19,709 N with full-length beams demonstrating the highest strength (Huang et al., 2019). The CSM-reinforced beams displayed superior flexural properties through peak load increases of 25% to 49%, with ETR136 showing the greatest improvement. The reinforced specimens displayed progressive failure with maintained residual strength through their ability to extend plastic deformation while reducing crack propagation and enhancing energy absorption, consistent with earlier findings on modular timber reinforcement effectiveness (Mamat et al., 2025; Wdowiak-Postulak et al., 2023).

The observations of strain and failure showed that CSM reinforcement helped to distribute stress throughout the beam depth but mechanical connectors continued to be areas of high stress. The unreinforced beams failed at or near the joints because of grain splitting, fiber crushing and bolt deformation (Wdowiak-Postulak et al., 2024). The reinforced specimens failed later than the unreinforced ones but still showed stress localization at the mechanical connections which determined the failure sequence. Segmented beams failed earlier than monolithic beams in both groups, indicating that segmentation is the main factor affecting structural vulnerability (Wang et al., 2024).

The research results demonstrate that both reinforcement methods and mechanical connection designs need optimization for modular timber systems particularly when used in portable and quick-deployment applications such as forest bridges (Schirotter et al., 2018). The determination of appropriate segment length requires finding a balance between transportation convenience and assembly needs and structural performance and load distribution. The main focus of joint engineering should be to maintain structural stiffness and load continuity while enabling disassembly and

reusability. The selected reinforcement materials must fulfill modular design criteria requirements by showing durability and field suitability. Huang et al. (2019) recommend future research to develop advanced connection systems that reduce stress concentrations and enhance beam segment force transmission. According to Wdowiak-Postulak et al. (2023), hybrid reinforcing technologies that integrate steel elements with fiber-reinforced polymers (FRP) show promise for extending structural durability. Wang et al. (2024) indicated that laboratory results need both numerical simulations and field-scale experimental validations to become applicable for real-world situations.

5 CONCLUSION

This research systematically investigated the combined effects of mechanical connections, CSM reinforcement, and segmentation on modular timber beam performance through comprehensive experimental analysis. The study provides critical quantitative evidence for optimizing modular timber systems in rapid-deployment applications such as forest bridges.

CSM reinforcement delivered substantial performance improvements across multiple structural parameters. A 49% load capacity increase (29,397 N vs 19,709 N) represented the highest enhancement observed, while a 27.1% stiffness improvement (1,014,000 N/m vs 798,000 N/m) and a 31% tensile strain reduction (3,693.58 $\mu\text{m}/\text{m}$ to 2,550.76 $\mu\text{m}/\text{m}$) demonstrated quantifiable stress redistribution and enhanced structural resilience.

Segmentation severely degraded performance in exponential patterns. Five-segment beams achieved only 50.5% of the continuous beam capacity (9,956 N vs 19,709 N), while three-segment non-reinforced beams experienced a 74.77% stiffness loss compared to 7.58% for continuous specimens. Segmentation beyond three segments resulted in >80% performance degradation in most configurations.

The three-segment reinforced configuration (ETR318) emerged as the optimal, achieving exceptional stiffness enhancement with an SDI of -34.03% - indicating progressive stiffness improvement rather than degradation. This represents a 108.8% performance differential compared to its non-reinforced counterparts (SDI = 74.77%), transforming the worst-performing unreinforced configuration into the best-performing reinforced system.

The research suggests quantitative performance thresholds in which SDI values <85% represent acceptable performance, 85–90% values require optimization, and >90% indicate structurally discouraged configurations. Three segments per 3.0-meter span represents

the critical design boundary where joint spacing enables optimal reinforcement engagement while maintaining practical modularity.

Mechanical connections consistently governed failure behavior, with timber-bolt interfaces experiencing stress concentrations leading to bearing failure and progressive joint degradation. Reinforced specimens maintained 22-35% residual capacity after peak loading, demonstrating superior post-peak behavior compared to <15% residual strength in non-reinforced beams.

These findings establish that effective modular systems require both optimized reinforcement strategies and segmentation limits. The three-segment threshold with mandatory CSM reinforcement enables practical modularity while preserving structural integrity for demanding applications.

Future research should incorporate cyclic loading, environmental durability testing, and advanced connection designs to further enhance modular timber system performance and expand applicability in sustainable infrastructure applications.

DISCLAIMER

The authors declare no conflict of interest.

ACKNOWLEDGMENTS

The authors would like to express their sincere gratitude to the Forest Research Institute Malaysia (FRIM) for providing the research facilities, materials, and technical support essential for conducting this study. Special appreciation is extended to Faculty of Civil Engineering, Universiti Teknologi MARA (UiTM) Shah Alam for the academic guidance and support throughout this research. This work was partially supported by the PhD research program at UiTM. The authors also thank the laboratory technicians and colleagues who assisted in the experimental setup and data collection.

REFERENCES

- ASTM International (2021a), 'D0198-21a standard test methods of static tests of lumber in structural sizes'. PA: ASTM International.
URL: <https://doi.org/10.1520/d0198-21a>
- ASTM International (2021b), 'D5652-21 standard test methods for single-bolt connections in wood and wood-based products'. PA: ASTM International.
URL: <https://doi.org/10.1520/d5652-21>
- Boafo, F. E., Kim, J.-H. and Kim, J.-T. (2016), 'Performance of Modular Prefabricated Architecture: Case

Study-Based Review and Future Pathways', *Sustainability* **8**(6), 558.

URL: <https://doi.org/10.3390/su8060558>

Chen, J., Wang, H., Yu, Y., Liu, Y. and Jiang, D. (2020), 'Loosening of Bolted Connections under Transverse Loading in Timber Structures', *Forests* **11**(8), 816.

URL: <https://doi.org/10.3390/f11080816>

Franke, S., Franke, B. and Harte, A. M. (2015), 'Failure modes and reinforcement techniques for timber beams – State of the art', *Construction and Building Materials* **97**, 2–13.

URL: <https://doi.org/10.1016/j.conbuildmat.2015.06.021>

Hu, Y., Wei, Y., Chen, S., Yan, Y. and Zhang, W. (2021), 'Experimental Study on Timber-Lightweight Concrete Composite Beams with Ductile Bolt Connectors', *Materials* **14**(10), 2632.

URL: <https://doi.org/10.3390/ma14102632>

Huang, H., Chang, W. and Chen, K. (2019), 'Study of SMA-dowelled timber connection reinforced by densified veneer wood under cyclic loading', *MATEC Web of Conferences* **275**, 1015.

URL: <https://doi.org/10.1051/mateconf/201927501015>

Karagiannis, V., Málaga-Chuquitaype, C. and Elghazouli, A. Y. (2016), 'Behaviour of hybrid timber beam-to-tubular steel column moment connections', *Engineering Structures* **131**, 243.

URL: <https://doi.org/10.1016/j.engstruct.2016.11.006>

Kržan, M., Pazlar, T. and Ber, B. (2023), 'Composite Beams Made of Waste Wood-Particle Boards, Fastened to Solid Timber Frame by Dowel-Type Fasteners', *Materials* **16**(6), 2426.

URL: <https://doi.org/10.3390/ma16062426>

Lee, S.-S., Park, K.-S., Jung, J.-S. and Lee, K.-S. (2020), 'Evaluation of the Structural Performance of a Novel Methodology for Connecting Modular Units Using Straight and Cross-Shaped Connector Plates in Modular Buildings', *Applied Sciences* **10**(22), 8186.

URL: <https://doi.org/10.3390/app10228186>

Liu, Y. and Xiong, H. (2018), 'Lateral performance of a semi-rigid timber frame structure: theoretical analysis and experimental study', *Journal of Wood Science* **64**(5), 591.

URL: <https://doi.org/10.1007/s10086-018-1727-7>

Lokaj, A., Dobeš, P. and Sucharda, O. (2020), 'Effects of Loaded End Distance and Moisture Content on the Behavior of Bolted Connections in Squared and Round Timber Subjected to Tension Parallel to the Grain', *Materials* **13**(23), 5525.

URL: <https://doi.org/10.3390/ma13235525>

Mamat, M. R., Hashim, M. H. M. and Nor, N. M. (2025), 'Reassessing Tension Side Reinforcement in Modular Timber Beams: Insights from Experimental Modal

Analysis in Forest Bridge Systems', *Jurnal Kejuruteraan* **37**(3), 1131–1144.

URL: [https://doi.org/10.17576/jkukm-2025-37\(3\)-05](https://doi.org/10.17576/jkukm-2025-37(3)-05)

Manalo, A. and Mutsuyoshi, H. (2011), 'Behavior of fiber-reinforced composite beams with mechanical joints', *Journal of Composite Materials* **46**(4), 483.

URL: <https://doi.org/10.1177/0021998311418263>

Mirski, R., Kuliński, M., Dziurka, D., Thomas, M. and Antonowicz, R. (2021), 'Strength Properties of Structural Glulam Elements from Pine (*Pinus sylvestris* L.) Timber Reinforced in the Tensile Zone with Steel and Basalt Rods', *Materials* **14**(10), 2574.

URL: <https://doi.org/10.3390/ma14102574>

Okunroumu, O., Salem, O. and Hadjisophocleous, G. (2022), 'Fire performance of hybrid mass timber beam-end connections with perpendicular-to-wood grain reinforcement', *Journal of Structural Fire Engineering* **13**(4), 433.

URL: <https://doi.org/10.1108/jsfe-06-2021-0036>

Rahman, M. J., Hasrul, M., Ashad, H., Yusuf, F. A. and Hasrul, N. R. (2024), 'An Assessment Of Derelict Building Constructions Situated In Coastal Regions', *Journal of the Civil Engineering Forum* **10**(3), 229.

URL: <https://doi.org/10.22146/jcef.10433>

Rebouças, A. S., Mehdipour, Z., Branco, J. M. and Lourenço, P. B. (2022), 'Ductile Moment-Resisting Timber Connections: A Review', *Buildings* **12**(2), 240.

URL: <https://doi.org/10.3390/buildings12020240>

Schiro, G., Giongo, I., Sebastian, W., Riccadonna, D. and Piazza, M. (2018), 'Testing of timber-to-timber screw-connections in hybrid configurations', *Construction and Building Materials* **171**, 170.

URL: <https://doi.org/10.1016/j.conbuildmat.2018.03.078>

Shi, D., Xu, Y., Demartino, C., Xiao, Y. and Spencer, B. F. (2023), 'Bio-based laminated truss structures with bolted steel connections: Experiment, modeling, and model-updating', *Earthquake Engineering & Structural Dynamics* **53**(2), 739.

URL: <https://doi.org/10.1002/eqe.4043>

Shu, Z., Ning, B., Chen, J., Li, Z., He, M., Luo, J. and Dong, H. (2022), 'Reinforced moment-resisting glulam bolted connection with coupled long steel rod with screwheads for modern timber frame structures', *Earthquake Engineering & Structural Dynamics* **52**(4), 845.

URL: <https://doi.org/10.1002/eqe.3789>

Wang, G., Xian, B., Ma, F. and Fang, S. (2024), 'Shear Performance of Prefabricated Steel Ultra-High-Performance Concrete (UHPC) Composite Beams under Combined Tensile and Shear Loads: Single Embedded Nut Bolts vs. Studs', *Buildings* **14**(8), 2425.

URL: <https://doi.org/10.3390/buildings14082425>

Wang, Y., Xia, J., Ma, R., Xu, B. and Wang, T. (2019), 'Experimental Study on the Flexural Behavior of an Innovative Modular Steel Building Connection with Installed Bolts in the Columns', *Applied Sciences* **9**(17), 3468.

URL: <https://doi.org/10.3390/app9173468>

Wdowiak-Postulak, A. (2020), 'Basalt Fibre Reinforcement of Bent Heterogeneous Glued Laminated Beams', *Materials* **14**(1), 51.

URL: <https://doi.org/10.3390/ma14010051>

Wdowiak-Postulak, A., Gocál, J., Bahleda, F. and Prokop, J. (2023), 'Load and Deformation Analysis in Experimental and Numerical Studies of Full-Size Wooden Beams Reinforced with Prestressed FRP and Steel Bars', *Applied Sciences* **13**(24), 13178.

URL: <https://doi.org/10.3390/app132413178>

Wdowiak-Postulak, A., Świt, G. and Dziedzic-Jagocka, I. (2024), 'Application of Composite Bars in Wooden, Full-Scale, Innovative Engineering Products—Experimental and Numerical Study', *Materials* **17**(3), 730.

URL: <https://doi.org/10.3390/ma17030730>

Yang, R., Li, H., Lorenzo, R., Ashraf, M., Sun, Y. and Yuan, Q. (2020), 'Mechanical behaviour of steel timber composite shear connections', *Construction and Building Materials* **258**, 119605.

URL: <https://doi.org/10.1016/j.conbuildmat.2020.119605>